JOURNAL OF BACTERIOLOGY, Sept. 2009, p. 5845–5848 Vol. 191, No. 18
0021-9193/09/$08.00+0 doi:10.1128/JB.00294-09

The CheZ Binding Interface of $CheA_S$ Is Located in α-Helix E[▽]

Christopher O'Connor,† Philip Matsumura, and Andres Campos*

Department of Microbiology and Immunology, College of Medicine, University of Illinois at Chicago, Chicago, Illinois 60612

Received 4 March 2009/Accepted 29 June 2009

Specific CheA-short ($CheA_S$) residues, L123 and L126, were identified as critical for CheZ binding. In the $CheA_S$ ′P1-CheZ nuclear magnetic resonance structure, these residues form an interaction surface on α-helix E in the ′P1 domain. Both L123 and L126 are buried in CheA-long ($CheA_L$), providing an explanation for why $CheA_L$ fails to bind CheZ.

The *cheA* gene is essential in the regulation of the chemotaxis cascade in *Escherichia coli*. It contains two tandem translation starts that encode CheA-long ($CheA_L$; 71 kDa) and CheA-short ($CheA_S$; 66 kDa) (8, 9, 16). $CheA_L$ is the histidine kinase responsible for phosphorylating the response regulator CheY. In turn, phosphorylated CheY is the form that binds to the flagellar motor switch complex, increasing the probability of reversal of flagellar rotation (from counterclockwise to clockwise). This event allows cells to reorient (tumble) and change the direction of their swimming. The dephosphorylation of CheY is enhanced by CheZ (the CheY phosphatase) and $CheA_S$ (20). Cells lacking CheZ fail to respond appropriately to attractant stimuli (3). It is known that CheZ localization to the polar chemoreceptor clusters requires $CheA_S$ (2, 17). $CheA_S$ interacts with CheZ through the C-terminal fragment of the P1 domain (residues 98 to 139). This domain of $CheA_S$ has been termed ′P1 and has been identified as the CheZ binding domain (10). The N terminus of $CheA_S$ lacks the first 97 amino acids present in the P1 domain of $CheA_L$, and it was postulated that these first 97 residues in $CheA_L$ mask the CheZ binding site (10). Recently, it has been reported that a low level of $CheA_L$ binding to CheZ in vivo can be detected by fluorescent resonance energy transfer (FRET) (6). However, we have not been able to detect this interaction by coimmunoprecipitation assays (20).

In this work, we describe *cheA* mutations that affect only the CheZ binding activity of $CheA_S$, since previous work demonstrated that the mutation of the $CheA_S$ gene start codon (corresponding to residue M98) not only prevents $CheA_S$ expression, but also affects $CheA_L$ signaling (14). Our data are consistent with the location of the $CheA_S$ binding surface for CheZ on α-helix E ($CheA_L$ nomenclature; Protein Data Bank identification number 1I5N).

Results from protein interaction by cysteine modification (PICM) assays suggested that CheZ binds to a region of α-helix E in ′P1 (10). To identify specific residues involved in CheZ binding, cysteine scanning mutagenesis in $CheA_S$ ′P1 was carried out. Various residues in the C120S mutant ′P1 domain ($'P1^{C120S}$) fused to glutathione *S*-transferase (GST) were replaced with cysteine by using the QuikChange site-directed mutagenesis kit (Stratagene) (Table 1).

The ′P1 constructs with cysteine substitutions were tested for their CheZ binding activities in GST coimmunoprecipitation assays as described previously (10). Protein lysates containing overexpressed GST-′P1 fusion constructs with cysteine substitutions and wild-type CheZ were mixed and incubated on ice for 1 h. Protein complexes were captured via centrifugation using glutathione agarose beads. Each complex was washed twice and eluted from the beads with glutathione. The L123C and L126C substitutions in ′P1 led to the loss of CheZ binding activity (Fig. 1). Residues L123 and L126 were predicted previously to participate in the ′P1/CheZ interaction (2). Constructs with other substitutions showed partial binding to CheZ. Of the substitutions in this group, Y118C and R124C conferred the greatest defects (Fig. 1). These results indicate that residues L123 and L126 lie within the region of ′P1 that interacts with CheZ.

Complementation of a Δ*cheA* strain (RP9535) (Table 1) by the L126A mutant form of CheA ($CheA^{L126A}$) was examined. Swarm plates containing 0.4 μM sodium salicylate as the inducer were used with a vector containing the P_{nah} promoter (Table 1) to ensure wild-type levels of expression. Plasmids carrying either *cheA* or *cheA*(*L126A*) complement a Δ*cheA* strain to equal degrees (data not shown). We conclude that the L126A substitution does not sufficiently affect CheA function to significantly affect chemotactic ring formation.

CheZ mutants with localization defects ($CheZ^{W97S}$ and $CheZ^{F98S}$) also support chemotaxis on swarm plates (2). However, $CheZ^{F98S}$ shows a poor response to increasing concentrations of attractant stimuli when observed in real time via FRET experiments (19). Since the loss of $CheA_S$/CheZ interaction failed to produce a significant chemotaxis defect on swarm agar, the rate of change of direction (RCD) for individual *cheA* mutant cells was calculated with computer-assisted motion analysis (by Motion Analysis, Inc.) to measure potential signaling defects due to the loss of $CheA_S$/CheZ interaction (13) (Fig. 2). Cells were induced at mid-logarithmic phase (optical density at 600 nm of ~0.5) with 4 μM sodium salicylate and incubated for an additional 1.5 h at 34°C. The cells were then diluted (1:3) with isotropic medium (unstimulated) or fresh tryptone broth (TB) medium (the addition of fresh nutrients provides an attractant stimulus). Isotropic medium

* Corresponding author. Mailing address: Molecular Biology Consortium, 835 S. Wolcott Ave. (M/C 790), MSB E-603, Chicago, IL 60612-7344. Phone: (312) 996-1216. Fax: (312) 413-2952. E-mail: acampos@uic.edu.

† Present address: Department of Cell Biology, Neurology and Anatomy, Loyola University Medical School, 2160 South First Ave., Bldg. 102, Maywood, IL 60153.

▽ Published ahead of print on 6 July 2009.

TABLE 1. Strains and plasmids

Strain or plasmid	Genotype, phenotype, and/or description	Source or reference
Strains		
RP437	*thr-1* (Am) *leuB6 his-4 metF159* (Am) *eda-50 rpsL356 thi-1 ara-14 mtl-1 xyl-5 tonA31 tsx-78 lacY1* F^-	11
RP9535	RP437 Δ*cheA*	J. S. Parkinson
RP1616	RP437 Δ*cheZ*	J. S. Parkinson
RP9543	RP437 Δ*cheA* Δ*cheZ*; lacks MCPs	J. S. Parkinson
Plasmids		
pKG110[a]	Cam^r P_{nah}; used for sodium salicylate induction of protein	J. S. Parkinson
pPA113	Cam^r; pKG110 derivative containing *cheA*	J. S. Parkinson
pOC100	Kan^r; pET24a(+) derivative containing *cheZ*	10
pOC407	Cam^r; pKG110 derivative containing *cheA*(*L126A*)	This study
pOC810	Pen^r; used for GST-′$P1^{C120S}$ overexpression	10
pOC824[b]	Pen^r; used for GST-′$P1^{C120S/E117C}$ overexpression	This study
pOC825[b]	Pen^r; used for GST-′$P1^{C120S/Y118C}$ overexpression	This study
pOC827[b]	Pen^r; used for GST-′$P1^{C120S/N121C}$ overexpression	This study
pOC829[b]	Pen^r; used for GST-′$P1^{C120S/L123C}$ overexpression	This study
pOC830[b]	Pen^r; used for GST-′$P1^{C120S/R124C}$ overexpression	This study
pOC831[b]	Pen^r; used for GST-′$P1^{C120S/Q125C}$ overexpression	This study
pOC832[b]	Pen^r; used for GST-′$P1^{C120S/L126C}$ overexpression	This study
pOC834[b]	Pen^r; used for GST-′$P1^{C120S/L128C}$ overexpression	This study
pOC835[b]	Pen^r; used for GST-′$P1^{C120S/E129C}$ overexpression	This study

[a] pKG110 allows the expression of genes from the sodium salicylate-inducible promoter P_{nah} from *Pseudomonas* spp.
[b] Site-directed mutagenesis was carried out in the GST-′$P1^{C120S}$ background (pOC810).

was prepared by centrifuging a sample of the culture, and the supernatant was used as a diluent. Under isotropic conditions, the RP9535 (Δ*cheA*) strain complemented with *cheA* showed wild-type swimming behavior (Fig. 2). The RCD values for the complemented Δ*cheA* strain were in the range from 600 to 800 degrees/s, as seen previously with wild-type bacteria (3, 7). RP1616 (Δ*cheZ*) showed tumbling behavior (RCD, ~1,500 degrees/s) (Fig. 2). Interestingly, the *cheA*(*L126A*) mutant exhibited an RCD (~1,200 degrees/s) higher than that of the wild type but not as high as that of the Δ*cheZ* mutant (Fig. 2).

The high RCD value corresponding to the L126A substitution potentially reflects the need for $CheA_S$-enhanced CheZ phosphatase activity at the receptor patches.

To see if cells expressing $CheA^{L126A}$ could respond to an attractant stimulus, the cells were diluted (1:3) in fresh TB medium, which induces a broad attractant stimulus due to the addition of new nutrients to the cells. As predicted, cells demonstrated lower RCD values that correlate with smooth, uninterrupted swimming patterns. Wild-type *E. coli*, as well as RP9535 complemented with *cheA*, exhibited a smooth swimming phenotype: RCD, ~400 degrees/s (Fig. 2). The Δ*cheZ* strain, as well as RP9535 complemented with *cheA*(*L126A*), demonstrated a lower RCD (~800 degrees/s) than that exhibited in isotropic medium. All of the changes were proportional to previous results for isotropic conditions. We conclude that the increase in the RCD of the L126A mutant strain compared to that of the wild type is due to the inability of $CheA^{L126A}$ to bind CheZ.

To facilitate the interpretation of the RCD data, the flagellar rotation patterns were analyzed. Tethered cells were grown and induced under exactly the same conditions used for motion analysis assays (see above). Cells were diluted (1:9) in isotropic medium, and flagella were disrupted from cells by passing the cells through a 25-gauge needle (~10 times). Antiflagellar serum (a gift from John S. Parkinson) was added to the cells, and the preparation was observed under a microscope. The protocol and the classification of the rotational behavior were carried out as described elsewhere (15). The observed behavior of the tethering cells corroborates the RCD data. Cells with wild-type behavior and those with smooth swimming patterns (Δ*cheA* cells) presented reversing and clockwise rotation, respectively, while the obtained RCDs ranged from 300 to 800 degrees/s. Cells with tumble behavior [Δ*cheA* cells complemented with *cheA*(*L126A*) and Δ*cheZ* cells] presented pre-

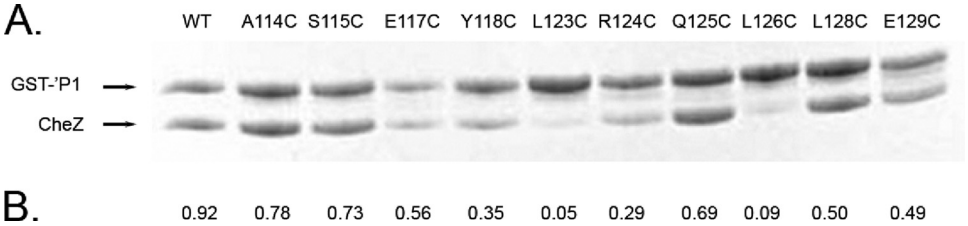

FIG. 1. Residues Y118, L123, R124, and L126 are involved in CheA ′P1/CheZ interactions. (A) Protein complexes isolated as described in the text were analyzed by sodium dodecyl sulfate–15% polyacrylamide gel electrophoresis and Coomassie blue staining. WT, wild type. (B) CheZ/GST-′P1 interaction ratios were calculated with the software ImageJ version 1.38m (1, 12). The wild-type CheZ/GST-′P1 interaction ratio is around 1. One representative result from two experiments is shown.

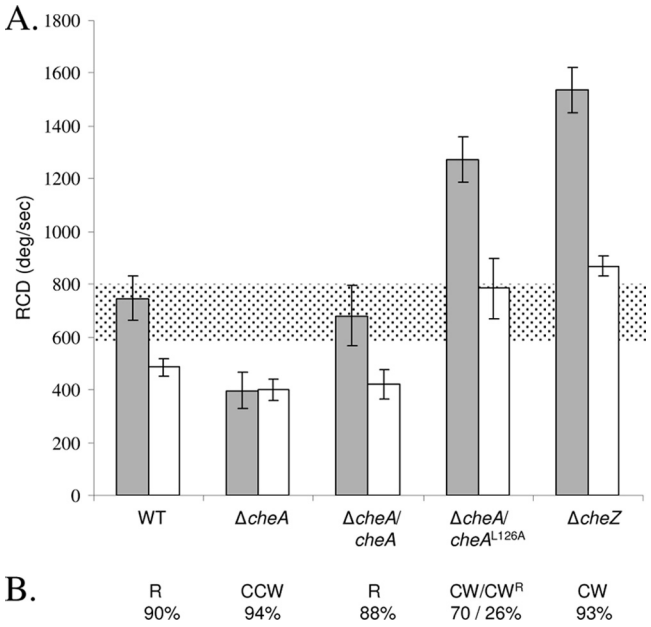

FIG. 2. RCDs for each CheA mutant strain without and with stimulation. (A) The RP9535 (Δ*cheA*) strain was transformed with *cheA* and *cheA*(*L126A*) pKG110 derivatives. Wild-type *E. coli* (RP437; WT) and a Δ*cheZ* strain (RP1616) were used as controls. Data were collected without stimulation (using isotropic medium) (gray bars) and with stimulation (using fresh medium) (white bars). As a control, RP9535 containing pPA113 was grown without an inducer (data not shown). The dotted region indicates the range of wild-type behavior (RCDs from 600 to 800 degrees/s) under these conditions. An RCD below 600 degrees/s indicates a smooth swimming pattern, and an RCD above 800 degrees/s indicates tumble behavior. Error bars indicate standard errors of the means ($n = 3$). Δ*cheA*/*cheA*, Δ*cheA* strain complemented with *cheA*; *cheA*/*cheA*^{L126A}, Δ*cheA* strain complemented with *cheA*(*L126A*). (B) Percentages of cells from each strain with the indicated flagellar rotation patterns are shown. R, reversing; CCW and CW, exclusively counterclockwise and clockwise, respectively; CW^R, reversing less frequently, with a clear bias toward the clockwise direction. The following numbers of total cells per strain were observed: WT, 104 cells; Δ*cheA* strain, 77 cells; Δ*cheA* strain complemented with *cheA*, 127 cells; Δ*cheA* strain complemented with *cheA*(*L126A*), 81 cells; and RP1616, 177 cells.

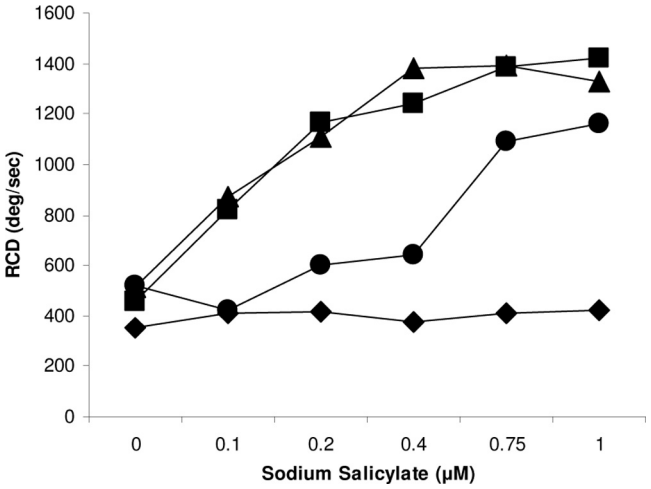

FIG. 3. Results from an in vivo functional assay show that the L126C substitution does not affect CheA$_L$ activity. RP9543 (Δ*cheA* Δ*cheZ* strain lacking MCPs) was transformed with the pKG110 vector as a control (◆) and with the *cheA* (■), *cheA*(*L126A*) (▲), and *cheA*(*M98I*) (●) pKG110 derivatives. RCDs for each strain and inducer concentration were calculated. One representative result from two experiments is shown.

dominantly or exclusively clockwise rotation and had RCDs higher than 800 degrees/s (Fig. 2).

An in vivo assay to test CheA$_L$ kinase function was used to determine whether the L126A substitution affects CheA$_L$ signaling activity (18). The effect of *cheA*(*L126A*) on swimming behavior was not due to protein expression or stability problems, since the CheA proteins from the wild-type and *cheA*(*L126A*) strains were present at the same levels (data not shown).

A strain (RP9543) lacking all of the major monocyte chemoattractant proteins (MCPs), as well as *cheA* and *cheZ*, was transformed with *cheA*, *cheA*(*M98I*), and *cheA*(*L126A*). Since this strain lacks MCPs, *cheA*, and *cheZ*, these cells can induce tumbles only if CheA$_L$ is reintroduced. The tumble frequency is directly correlated to an increase in the concentration of CheA$_L$ and phosphotransfer to CheY (18). If a variant of CheA$_L$ is unable to undergo autophosphorylation and subsequent phosphotransfer to CheY, then the strain will not present a tumbling phenotype. Cells were grown to mid-log phase and then induced with different concentrations of sodium salicylate. After 1.5 h, the cells were diluted (1:3) with isotropic medium. As the concentration of wild-type CheA$_L$ increased, the RCD increased to values indicative of tumbling behavior (Fig. 3). The strain containing *cheA*(*M98I*) failed to reach the same level of tumbling behavior as the strain containing wild-type CheA, consistent with the notion that the M98I substitution disrupts CheA$_L$ signaling (14). The strain carrying the L126A substitution showed the same level of activity as the wild type (Fig. 3). The L126A substitution does not affect CheA$_L$ autophosphorylation and phosphotransfer activities; therefore, the L126A phenotype depicted in Fig. 2 is due to a loss in CheZ binding activity.

The behavioral defect conferred by *cheA*(*L126A*) represents a phenotype associated with the CheA$_S$/CheZ interaction. The mutant protein lacks the ability to interact with CheZ, which may lead to lower phosphatase activity. These results are in agreement with previous observations that the *cheZ*(*F98S*) protein fails to interact with CheA$_S$ and responds weakly to an attractant stimulus (2). Cells containing *cheA*(*L126A*) also respond poorly to a broad attractant stimulus [compare the responses of wild-type *cheA* and *cheA*(*L126A*) mutant cells depicted in Fig. 2].

The cysteine scanning data were mapped onto the ′P1 structure (Fig. 4). In the nuclear magnetic resonance structure of CheZ and CheA$_S$ (5), α-helix E of CheA$_S$ binds directly to CheZ. The residues in ′P1 critical for CheZ binding activity (L123 and L126) appear on the same surface of α-helix E as C120 (Fig. 4), in an area of ′P1 previously identified as important for CheZ binding activity (10). The relative solvent accessibilities of residues L123 and L124 in both CheA P1 (Protein Data Bank identification number 1I5N) and CheA ′P1 (5) were calculated with the DeepView Swiss-PdbViewer (4). In the CheA$_L$ structure, residues L123 and L126 are buried in the five-α-helix bundle (α-helices A to E), presenting solvent ac-

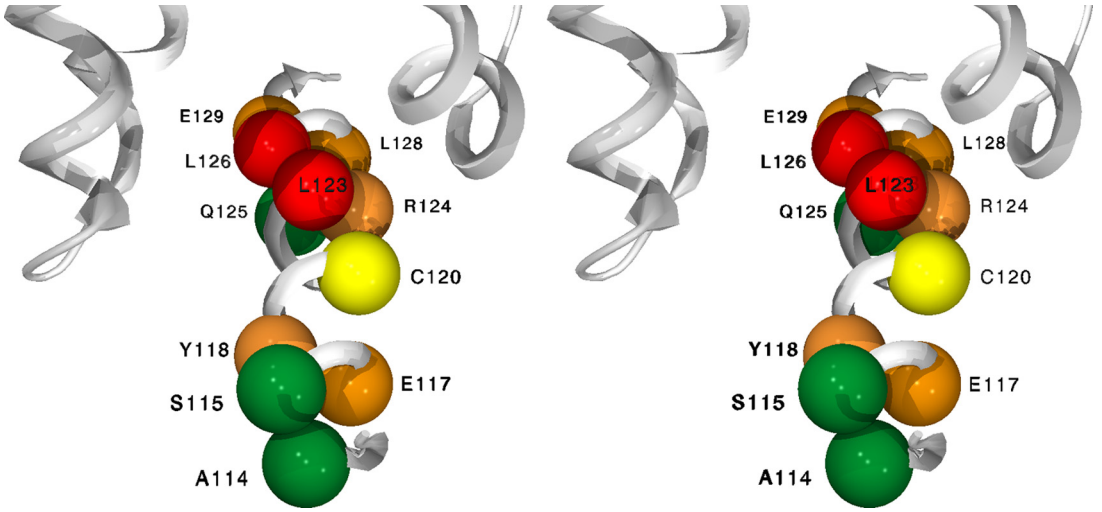

FIG. 4. CheA ′P1 residues involved in CheZ binding map to a single interface surface. The nuclear magnetic resonance model structure of $CheA_S$ bound to CheZ (5) was used to map the residues in $CheA_S$. In this stereoschematic diagram, the region comprising residues D112 to L131 of CheA ′P1 (α-helix E) is shown as a ribbon. A partial CheZ structure is also shown as ribbons (top). Alpha carbons of the residues in α-helix E of CheA that were changed to cysteine and affect CheZ binding are shown as spheres. Residues that have partial CheZ binding when changed to cysteine are shown in green (for ratios from 0.69 to 0.78) (Fig. 1) and orange (for ratios from 0.25 to 56). In red are L123 and L126, the replacement of which with cysteine causes the loss of interaction with CheZ (ratio < 0.1). The residue at position 120 (yellow) was previously shown to be capable of binding CheZ when cysteine is mutated to serine. When C120 is labeled with fluorescein 5-maleimide, CheZ binding is lost (10). The stereomodel figure was prepared with Swiss-PdbViewer v3.7 (4) (software from http://www.expasy.org/spdbv/) and rendered with POV-Ray 3.1 (software from http://povray.org/).

cessibilities of 0 and 4%, respectively, whereas in $CheA_S$ ′P1, these residues are exposed (with solvent accessibilities of 36% for L123 and 32% for L126) to allow interaction with the CheZ dimer. These results show that these two residues critical for CheZ binding activity are masked in the P1 domain of $CheA_L$, which prevents $CheA_L$ from interacting with CheZ.

We thank F. W. Dahlquist for the coordinates of the CheZ-$CheA_S$ model and J. S. Parkinson for kindly supplied antiflagellar serum. We also acknowledge Peggy O'Neill for critical reading of the manuscript.

This work was supported by National Institutes of Health grant GM062044 to P.M.

REFERENCES

1. **Abramoff, M. D., P. J. Magelhaes, and S. J. Ram.** 2004. Image processing with ImageJ. Biophotonics Int. **11:**36–42.
2. **Cantwell, B. J., R. R. Draheim, R. B. Weart, C. Nguyen, R. C. Stewart, and M. D. Manson.** 2003. CheZ phosphatase localizes to chemoreceptor patches via CheA-short. J. Bacteriol. **185:**2354–2361.
3. **Dowd, J. P., and P. Matsumura.** 1997. The use of flash photolysis for a high-resolution temporal and spatial analysis of bacterial chemotactic behaviour: CheZ is not always necessary for chemotaxis. Mol. Microbiol. **25:** 295–302.
4. **Guex, N., and M. C. Peitsch.** 1997. SWISS-MODEL and the Swiss-PdbViewer: an environment for comparative protein modeling. Electrophoresis **18:**2714–2723.
5. **Hao, S., D. Hamel, H. Zhou, and F. W. Dahlquist.** 2009. Structural basis for the localization of the chemotaxis phosphatase CheZ by CheA-short. J. Bacteriol. **191:**5842–5844.
6. **Kentner, D., and V. Sourjik.** 2009. Dynamic map of protein interactions in the *Escherichia coli* chemotaxis pathway. Mol. Syst. Biol. **5:**238.
7. **Khan, S., F. Castellano, J. L. Spudich, J. A. McCray, R. S. Goody, and G. P. Reid.** 1993. Excitatory signaling in bacteria probed by caged chemoeffectors. Biophys. J. **65:**2368–2382.
8. **Kofoid, E. C., and J. S. Parkinson.** 1991. Tandem translation starts in the *cheA* locus of *Escherichia coli*. J. Bacteriol. **173:**2116–2119.
9. **Matsumura, P., M. Silverman, and M. I. Simon.** 1977. Synthesis of *mot* and *che* gene products of *Escherichia coli* programmed by hybrid ColE1 plasmids in minicells. J. Bacteriol. **132:**996–1002.
10. **O'Connor, C., and P. Matsumura.** 2004. The accessibility of Cys-120 in $CheA_S$ is important for the binding of CheZ and enhancement of CheZ phosphatase activity. Biochemistry **43:**6909–6916.
11. **Parkinson, J. S., and S. E. Houts.** 1982. Isolation and behavior of *Escherichia coli* deletion mutants lacking chemotaxis functions. J. Bacteriol. **151:**106–113.
12. **Rasband, W. S.** 2008. ImageJ. National Institutes of Health, Bethesda, MD. http://rsb.info.nih.gov/ij/.
13. **Sager, B. M., J. J. Sekelsky, P. Matsumura, and J. Adler.** 1988. Use of a computer to assay motility in bacteria. Anal. Biochem. **173:**271–277.
14. **Sanatinia, H., E. C. Kofoid, T. B. Morrison, and J. S. Parkinson.** 1995. The smaller of two overlapping *cheA* gene products is not essential for chemotaxis in *Escherichia coli*. J. Bacteriol. **177:**2713–2720.
15. **Slocum, M. K., and J. S. Parkinson.** 1985. Genetics of methyl-accepting chemotaxis proteins in *Escherichia coli*: null phenotypes of the *tar* and *tap* genes. J. Bacteriol. **163:**586–594.
16. **Smith, R. A., and J. S. Parkinson.** 1980. Overlapping genes at the *cheA* locus of *Escherichia coli*. Proc. Natl. Acad. Sci. USA **77:**5370–5374.
17. **Sourjik, V., and H. C. Berg.** 2000. Localization of components of the chemotaxis machinery of *Escherichia coli* using fluorescent protein fusions. Mol. Microbiol. **37:**740–751.
18. **Tawa, P., and R. C. Stewart.** 1994. Mutational activation of CheA, the protein kinase in the chemotaxis system of *Escherichia coli*. J. Bacteriol. **176:**4210–4218.
19. **Vaknin, A., and H. C. Berg.** 2004. Single-cell FRET imaging of phosphatase activity in the *Escherichia coli* chemotaxis system. Proc. Natl. Acad. Sci. USA **101:**17072–17077.
20. **Wang, H., and P. Matsumura.** 1996. Characterization of the $CheA_S$/CheZ complex: a specific interaction resulting in enhanced dephosphorylating activity on CheY-phosphate. Mol. Microbiol. **19:**695–703.